Fermi National Accelerator Laboratory

FERMILAB-Conf-00/080-E
CDF

New Physics with CDF in Run I and Run II

A. Nomerotski
For the CDF Collaboration

University of Florida
Gainesville, Florida 32611

Fermi National Accelerator Laboratory
P.O. Box 500, Batavia, Illinois 60510

April 2000

Presented at and to appear in the Published Proceedings of the *7th International Symposium on Particles, Strings and Cosmology (PASCOS 99)*, Granlibakken, Tahoe City, California, December 10-16, 1999

Operated by Universities Research Association Inc. under Contract No. DE-AC02-76CH03000 with the United States Department of Energy

CDF NOTE 5270

NEW PHYSICS WITH CDF IN RUN I AND RUN II

ANDREI NOMEROTSKI
University of Florida, Gainesville, 32611 USA
E-mail: nomerot@fnal.gov

We present here recent CDF searches for new phenomena in Run I data. The scalar top and scalar bottom quarks searches are described in the framework of supersymmetric models. We also discuss CDF limits on the Higgs boson and continuum and resonantly produced leptoquarks. Run II starting in March 2001 will allow us to considerably improve the Tevatron reach in all these channels.

1 Supersymmetric Top and Bottom Searches

The Tevatron is the world largest $p\bar{p}$ collider at Fermilab with the 1.8 TeV center of mass energy. During Run I in 1992-1996 the DØ and CDF [1] detectors accumulated over 100 pb^{-1} of data per experiment. The high energy of collisions and the large accumulated luminosity make new phenomena searches with these detectors especially interesting.

In this section we describe the CDF searches for the supersymmetric partners of the top and bottom quarks. Supersymmetry (SUSY) [2] assigns to each Standard Model (SM) particle a superpartner with a spin different by 1/2. Here, we assume that R-parity is conserved and, therefore, the Lightest Supersymmetric Particle (LSP) is stable. Stable neutral LSP escapes the detector undetected giving the classic SUSY signature at the hadron colliders : missing transverse energy ($\not\!\!E_T$). In SUSY the SM quark helicity states q_L and q_R acquire scalar partners $\tilde{q}_L$ and $\tilde{q}_R$. Most models predict that the masses of the first two generations of scalar quarks are approximately degenerate. The scalar top quark ($\tilde{t}$) mass, however, may be lower than that of the other scalar quarks due to a substantial Yukawa coupling resulting from the large top quark mass. In addition, mixing between $\tilde{t}_L$ and $\tilde{t}_R$ can cause a large splitting between the mass eigenstates [3]. Thus, the $\tilde{t}$ has a good chance to be the lightest scalar quark. Similarly, in some regions of supersymmetric parameter space (large $\tan\beta$) a large mixing can cause a significant splitting between mass eigenstates of the scalar bottom quark.

At the Tevatron, the third generation scalar quarks are strongly produced in pairs via gg and $q\bar{q}$ fusion. We first report the CDF search for $\tilde{t}_1 \to c\tilde{\chi}^0_1$ [4]. This decay proceeds via a one-loop diagram and will become dominant when the tree-level decay $\tilde{t}_1 \to b\tilde{\chi}_1^+$ is kinematically forbidden. For the scalar bottom quark search the $\tilde{b}_1 \to b\tilde{\chi}_1^0$ decay mode was considered which dominates over most of the parameter space. $\tilde{t}\bar{\tilde{t}}$ production will result in two charm jets, while $\tilde{b}\bar{\tilde{b}}$ in two bottom jets with a significant $\not{E}_T$ present in both reactions.

Events with 2 or 3 jets with $E_T \geq 15$GeV and $|\eta| \leq 2$ were selected, requiring that there are no other jets in the event with $E_T \geq 7$GeV and $|\eta| \leq 3.6$. The $\not{E}_T$ cut was increased to 40 GeV, beyond the trigger threshold of 35 GeV. To reduce the contribution from processes where missing energy comes from jet energy mismeasurement, we required that the $\not{E}_T$ direction is neither parallel to any jet nor anti-parallel to the leading E_T jet : $min\Delta\phi(\not{E}_T, j) > 45°$, $\Delta\phi(\not{E}_T, j_1) < 165°$, and $45° < \Delta\phi(j_1, j_2) < 165°$. Events with one or more identified electrons (muons) with $E_T(P_T) > 10$ GeV(GeV/c) were rejected.

The dominant source of background for this analysis is the production of W+jets, where the W decays to a neutrino (leading to missing energy) and an electron or muon that is not identified, or a τ which decays hadronically.

The lifetime information is used to tag heavy flavor jets. For each track the probability that the track comes from the primary vertex is determined taking into account the impact parameter resolution. The combination of track probabilities for tracks associated to a jet is called *jet probability.* By construction, the jet probability is flat for a primary jet data sample. For bottom and charm jets, jet probability peaks near 0. To select charm jets for the scalar top search analysis we required that at least one jet has a probability of less than 0.05. This cut rejects about 97% of the background while its efficiency for the signal is about 25%. For bottom jet selection in the scalar bottom search, the signal significance is optimized by requiring that at least one jet has a probability of less than 0.01.

In the scalar top analysis, 11 events were selected in data, which is consistent with 14.5 ± 4.2 events expected from standard model processes. The null result in the scalar top search is interpreted as an excluded region in the $m_{\tilde{t}_1}$ - $m_{\tilde{\chi}_1^0}$ parameter space as shown in the left plot of Figure 1. In the scalar bottom analysis 5 events are selected with an expected background of 5.8 ± 1.8. The excluded region in $m_{\tilde{b}_1}$ - $m_{\tilde{\chi}_1^0}$ parameter space is shown in the right plot of Figure 1.

Another scalar top decay scenario considered by CDF is $\tilde{t}_1 \to bl\tilde{\nu}$ [5]. Here, $\tilde{\nu}$ is a scalar neutrino playing the role of LSP. A branching ratio of 33% is assumed for each $l = e,\ \mu,\ \tau$.

The $\tilde{t}_1$ signature for this channel is at least one isolated lepton, at least one b-jet and $\not{E}_T$. This signature is very similar to that of the top quark, with kinematic differences due to the smaller $\tilde{t}_1$ mass in our search region and the presence of two massive LSPs in the final state. We selected events with an

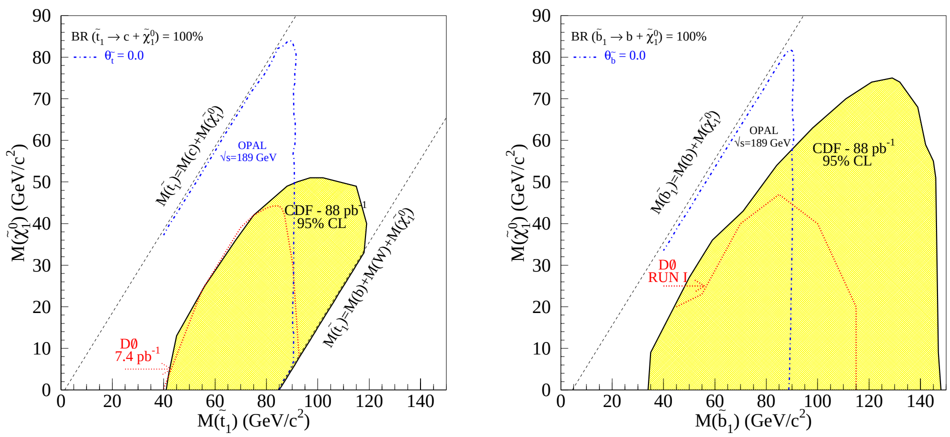

Figure 1. Left plot: CDF 95% CL exclusion region in $m_{\tilde{\chi}_1^0} - m_{\tilde{t}_1}$ plane for $\tilde{t}_1 \rightarrow c\tilde{\chi}_1^0$. Right plot: CDF 95% CL exclusion region in $m_{\tilde{\chi}_1^0} - m_{\tilde{b}_1}$ plane for $\tilde{b}_1 \rightarrow b\tilde{\chi}_1^0$.

electron with $E_T \geq 10$ GeV or muon with $p_T \geq 10$ GeV/c, $\not\!\!E_T \geq 25$ GeV and at least two jets, one with $E_T \geq 12$ GeV and the second with $E_T \geq 8$ GeV.

Events with at least one secondary vertex from b decays identified in the silicon vertex detector were required. The Drell-Yan background was reduced by removing events with two isolated, opposite-sign leptons. The background from $b\bar{b}$ events and events with hadrons misidentified as leptons (fake leptons) was lessened by requiring that the $\Delta\phi$ between the $\not\!\!E_T$ and the nearer of the two highest-E_T jets be ≥ 0.5 rad. The number of events remaining in our sample after all cuts is 81 while we expected 87.3 ± 8.8 background events. The most important backgrounds are $W(\rightarrow l\nu) + \geq 2$ jet with 45 events expected, $t\bar{t}$ (18 events) and fake leptons (13 events).

Unbinned likelihood fit of the H_T distribution was employed to determine the number of potential signal events. H_T is the scalar sum of lepton E_T, $\not\!\!E_T$ and jet E_T for all jets with $E_T \geq 8$ GeV. Fit results were consistent with zero signal in all considered mass points. The region excluded at 95% CL in the plane $m_{\tilde{t}_1}$ versus $m_{\tilde{\nu}}$ is shown in the left plot of Figure 2.

All results discussed in this section present a considerable extention of limits on scalar quarks set by LEP experiments.

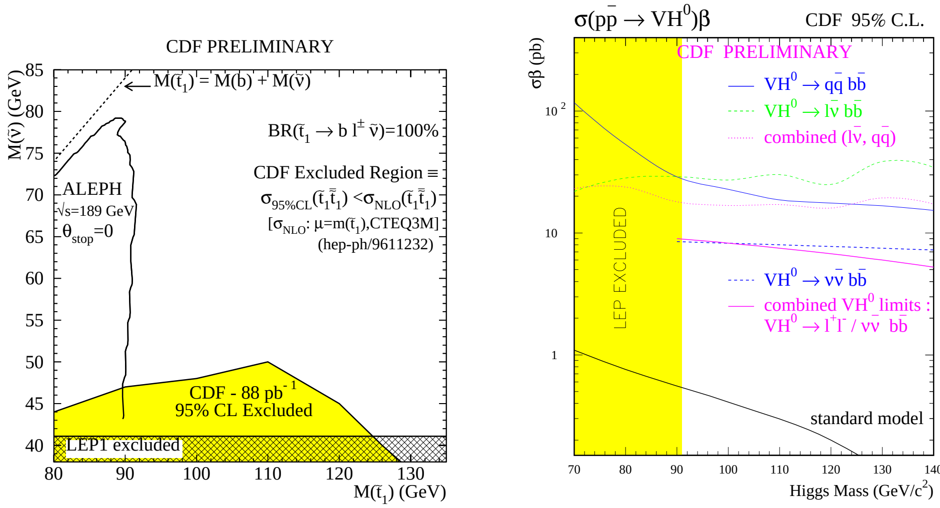

Figure 2. Left plot: CDF 95% CL exclusion region in $m_{\tilde{\nu}}$ – $m_{\tilde{t}_1}$ plane for $\tilde{t}_1 \to bl\tilde{\nu}$. Right plot : Compilation of the SM Higgs cross section limits. The best individual limit is obtained for $ZH \to b\bar{b}\nu\bar{\nu}$.

2 Higgs Searches

Higgs bosons produced in association with vector boson ($q\bar{q} \to V^* \to VH(V = W, Z)$) provide the most sensitive channels for Higgs searches at the Tevatron. The process $gg \to H$ is the dominant production mechanism, but has prohibitively large QCD background if one is looking for $H \to b\bar{b}$.

The new CDF Higgs search explores the process $q\bar{q} \to ZH \to (\nu\bar{\nu})(b\bar{b})$. The decay $Z \to \nu\bar{\nu}$ accounts for 19% of all possible decays modes of Z, while BR($H \to b\bar{b}$) decreases from 0.85 to 0.60 as the Higgs mass increases from 90 to 130 GeV/c^2. The same $\not\!\!E_T$ data sample has been employed as for the stop and sbottom searches described above. Events with $\not\!\!E_T > 40$ GeV and two or three jets of $E_T > 15$ GeV and $|\eta| < 2$ were selected. The contribution from processes where missing energy comes from jet energy mismeasurement was reduced requiring that the $\not\!\!E_T$ direction is not parallel to any jet with $E_T > 8$ GeV: $min\ \Delta\phi(\not\!\!E_T, j) > 57°$ and that $\Delta\phi(j_1, j_2) < 150°$. Events with isolated lepton or track with $E_T(P_T) > 10$ GeV(GeV/c) were rejected. b-jets were identified by the reconstructed secondary vertex. We observed 40 events with single b-tag and 4 events with double b-tags in good agreement with expectations. The most important sources of background, QCD and W/Z +heavy flavor production, are expected to contribute respectively 26 and 10 events to the total of 39 ± 4 in the single tag sample and 1.9 and 1.0 events to the total of 3.9 ± 0.6 in the double tag sample.

Employing a combination of the counting experiment and the maximum likelihood fits of the dijet mass distribution we set 95% CL upper limit on $\sigma(p\bar{p} \rightarrow ZH) \times Br(H \rightarrow b\bar{b})$ ranging from 9 to 7 pb as the Higgs mass varies from 90 to 130 GeV/c^2. The compilation of CDF cross section limits on the SM Higgs production is shown in the right plot of Figure 2. The channel $ZH \rightarrow (\nu\bar{\nu})(b\bar{b})$ gives the best individual cross section limit among all Higgs searches at CDF, though no mass limits can be set with Run I data.

3 Leptoquark Searches

Leptoquarks (LQ) are new particles with a direct coupling to a quark and a lepton predicted by various theories of Grand Unification [6]. In the case of vector LQs the Yang-Mills type couplings may be supplemented by anomalous couplings depending on two parameters k and λ. They are related to the anomalous 'magnetic' dipole moment and 'electric' quadrapole moment of the LQs in the color field. In the following we consider the cases of purely Yang-Mills type of coupling with k=0 and λ=0, and the minimal vector coupling with k=1 and λ=0. The phenomenological parameter β determines the decay branching fraction of LQ. $\beta = 1$ corresponds to a 100% decay branching fraction to a quark and a charged lepton.

CDF performed a search for third generation LQs with charge -1/3 or +1/3 decaying to $\nu_\tau b$ and the second generation LQs with charge +2/3 or -2/3 decaying to $\nu_\mu c$ [7]. Both decay modes assume $\beta = 0$. Final states which contain two heavy flavor jets (c-jets/b-jets for second/third generations of LQ), large missing energy (from neutrinos), and no high-p_T leptons were searched. This is exactly the same signature as in the CDF $\tilde{t} \rightarrow c\tilde{\chi}^0$ and $\tilde{b} \rightarrow b\tilde{\chi}^0$ searches discussed above. The selections and the data sample used for those analyses can be used to determine 95% CL cross section limits on the LQ production. The efficiency to the signal ranges from 3% to 7% for the $\nu_\mu c$ channel and from 6% to 13% for the $\nu_\tau b$ channel (for m$_{LQ}$ from 100 to 300 GeV/c^2).

The left plot in Figure 3 shows the CDF 95% CL cross section limit on $LQ_2 \rightarrow \nu_\mu c$ and on $LQ_3 \rightarrow \nu_\tau b$ together with the expected theoretical cross sections for scalar and two types of vector LQs. In the case of second generation leptoquarks we exclude scalar leptoquarks with $M < 123$ GeV/c^2, minimally coupled vector leptoquarks with $M < 171$ GeV/c^2, and Yang-Mills vector leptoquarks with $M < 222$ GeV/c^2. Similarly, in the case of third generation leptoquarks, we exclude scalar leptoquarks with $M < 148$ GeV/c^2, minimally coupled vector leptoquarks with $M < 199$ GeV/c^2, and Yang-Mills vector leptoquarks with $M < 250$ GeV/c^2.

Enhancement to leptoquark pair production could occur through the decay of technicolor resonance states. In one of the formulations of technicolor theory, a complete family of technifermions composed of an isodoublet of color triplet techniquarks and an isodoublet of color singlet technileptons form a rich spectrum of technimesons [8]. Combinations of techniquarks form color octet technirhos, ρ_{T8}, some of which have the same quantum numbers as the gluon. Color triplet technipions, which couple in a Higgs-like fashion to quarks and leptons and thus are expected to decay into heavy fermion pairs are identified as scalar leptoquarks of the third generation, π_{LQ}.

For scalar leptoquark production via color octet technirho decay, the ρ_{T8} will appear in s-channel modes coupling directly to the gluon. The leading-order cross section for leptoquark pair production from technirho resonance depends upon the technirho and leptoquark masses and the mass difference between color octet and triplet technipion $\Delta M = M(\pi_{T8}) - M(\pi_{LQ})$. The expected mass difference of 50 GeV/c^2 is determined by QCD corrections to the color octet and triplet technipion masses.

In this search we interprete the results of the third generation LQ analysis discussed above for the process $\rho_{T8} \to \pi_{LQ}\bar{\pi}_{LQ} \to b\bar{b}\nu_\tau\bar{\nu}_\tau$. Comparing the 95% CL cross section limit for $\pi_{LQ}\bar{\pi}_{LQ}$ production with theoretical predictions [9], we find 95% CL exclusion regions in the $M(\rho_{T8}) - M(\pi_{LQ})$ plane as shown in the right plot in Figure 3.

4 Run II expectations

For most of the next decade, the Fermilab Tevatron collider will define the high energy frontier of particle physics. The first stage of Run II, scheduled to begin in March 2001, will deliver at least 2 fb^{-1} of integrated luminosity per experiment at 2.0 TeV center-of-mass energy. This is more than 10 times the luminosity delivered in previous collider runs at 1.8 TeV.

Major upgrades of the both Tevatron detectors are under way. The most important improvements for CDF will be the new silicon microvertex detector and central drift chamber, extra muon coverage, new plug calorimeter and time-of-flight system. New design of the deadtimeless electronics will allow operations with 132 nsec time between collisions. The heavy flavor identification capabilities of the new CDF silicon tracker will be increased by a factor of about 2 for single tagging. Among other features, the detector will have

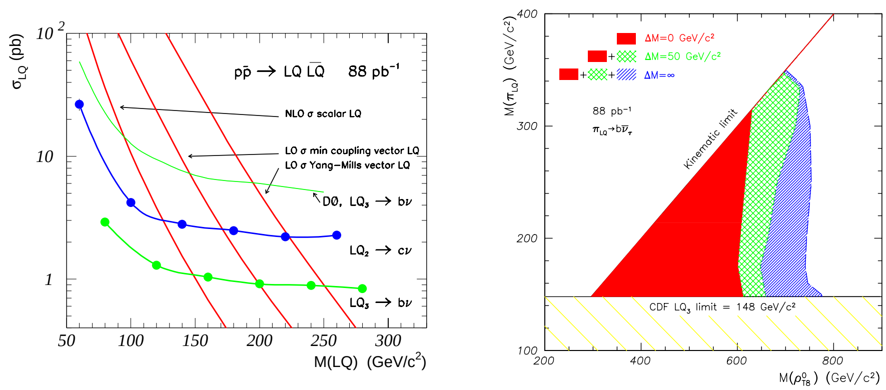

Figure 3. Left plot : CDF 95% CL cross section limit on $LQ_2 \to \nu_\mu c$ and on $LQ_3 \to \nu_\tau b$ together with the expected theoretical cross sections for scalar and two types of vector LQs. Right plot : CDF 95% CL exclusion regions in the $M(\rho_{T8}) - M(\pi_{LQ})$ plane.

the ability to trigger on displaced vertices from bottom and charm decays.

Searches for new phenomena is the main priority for Run II. A lot of work has been done to understand the reach for new physics in the future run [10]. We review projections for those channels which were discussed in this paper.

Left plot in Figure 4 shows the expected coverage of the $m_{\tilde{t}_1}$ - $m_{\tilde{\chi}^0_1}$ parameter space for 2 fb^{-1} in various channels [11]. Most of the channels will have sensitivity in the $\tilde{t}$ mass up to the top mass. Right plot in Figure 4 shows Run II projections for the continuum and resonantly produced leptoquarks of the third generation [12]. The sensitivity to the ρ_{T8} mass will be extended to approximately 1 TeV/c^2 in this channel.

Acknowledgments

We thank the organizers of the conference, the Fermilab staff and the technical staffs of the participating institutions for their interest and vital contributions. This work was supported by the U.S. Department of Energy and National Science Foundation; the Italian Istituto Nazionale di Fisica Nucleare; the Ministry of Education, Science, Sports and Culture of Japan; the Natural Sciences and Engineering Research Council of Canada; the National Science Council of the Republic of China; the Swiss National Science Foundation; the A. P. Sloan Foundation; the Bundesministerium fuer Bildung und Forschung,

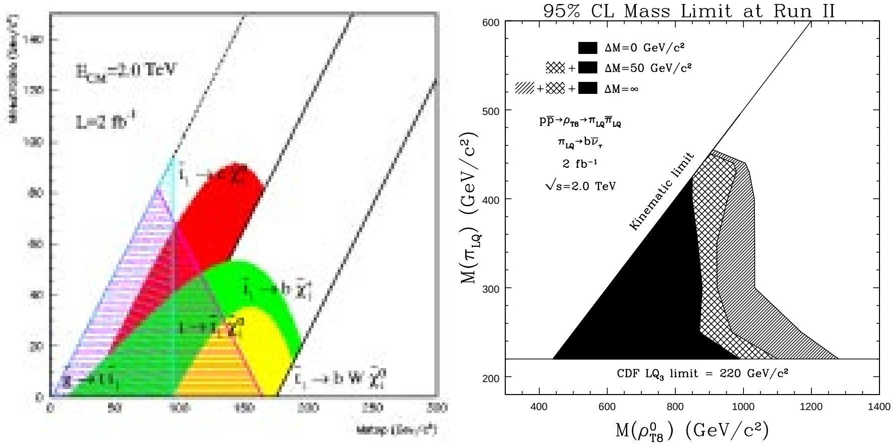

Figure 4. Left plot : Expected coverage of the $m_{\tilde{t}_1}$ - $m_{\tilde{\chi}_1^0}$ parameter space for 2 fb^{-1}. Gaugino unification is assumed for the chargino mass. Right plot : Run II projections for the continuum and resonantly produced leptoquarks of the third generation.

Germany; and the Korea Science and Engineering Foundation.

References

1. F. Abe *et al.* [CDF Collaboration], Nucl. Instr. Meth. **A271**, 387 (1988).
2. For reviews of SUSY see H. P. Niles, *Phys. Rev.* D **110**, 1 (1984); H. E. Haber and G. L. Kane, *Phys. Rev.* D **117**, 75 (1985).
3. H. Baer *et al.*, Phys. Rev. **D44**, 725 (1991).
4. F. Abe *et al.* [CDF Collaboration], hep-ex/9910049.
5. F. Abe *et al.* [CDF Collaboration], hep-ex/9912018.
6. see for example, J.C.Pati and A.Salam, *Phys. Rev.* D **8**, 1240 (1973); H.Georgi and S.L.Glashow, *Phys. Rev. Lett.* **32**, 438 (1974).
7. F. Abe *et al.* [CDF Collaboration], hep-ex/0004003.
8. E. Farhi and L. Susskind, Phys. Rev. **D20**, 3404 (1979).
9. K. Lane and M. Ramana, Phys. Rev. **D44**, 2678 (1991).
10. see http://fnth37.fnal.gov/susy.html
11. R.Demina, J.D.Lykken, K.T.Matchev and A.Nomerotski, hep-ph/9910275.
12. see http://runIIcomputing.fnal.gov/strongdynamics/web/strongdynamics.html